Fire Technology, 56, 639–672, 2020

Manufactured in The United States
https://doi.org/10.1007/s10694-019-00894-w

Full-Scale Informal Settlement Dwelling Fire Experiments and Development of Numerical Models

A. Cicione and R. S. Walls*, Department of Civil Engineering, Stellenbosch University, Stellenbosch, South Africa*

M. Beshir and D. Rush, School of Engineering, University of Edinburgh, Edinburgh EH9 3JL, UK*

Received: 21 May 2019/**Accepted:** 12 July 2019

Abstract. While fire-related injuries and deaths decreased in the global north over the past few years, they have increased in the global south. With more than one billion people residing in informal settlements (sometimes known as slums, ghettos or shantytowns), it is necessary that greater effort be placed on addressing and developing means for improving fire safety in these areas. As a result of advances made in computer technologies, emerging performance-based regulations and an increase in building complexity in the global north, the use of computer models simulating enclosure fires have increased dramatically. In this work an experimental investigation is presented for (a) a full-scale corrugated steel sheeting clad informal dwelling experiment and (b) a full-scale timber clad informal dwelling experiment. The experimental results are then compared to numerical models consisting of both simple two-zone (OZone) and computational fluid dynamic models. Currently, there is negligible literature available on Fire Dynamic Simulator (FDS) modelling of informal settlement dwellings (sometimes known as shacks or shanties) fires. This paper evaluates the plausibility of using FDS v6.7 and zonal models to predict certain fire parameters (i.e. ceiling temperatures, heat fluxes, etc.) for Informal Settlement Dwellings (ISDs) and to study the plausibility of using FDS to estimate the probability of fire spread. In this paper an introduction to ISDs is given with details pertaining to construction materials and considerations needed for numerical modelling of informal dwellings (i.e. thin permeable boundaries or combustible boundaries). Models are based upon (a) a prescribed heat release rate per unit area in FDS using data obtained from a Fire Propagation Apparatus test, and (b) an empirical two-zone model using OZone. The FDS validation guide was used to quantify the model uncertainties in order to give a critical separation distance at which fire spread between dwellings will not occur. It was found that at 3 m spacing between ISDs there is a 6% chance (based on the model uncertainties) that fire spread can occur. This is an important finding that highlights the danger associated with these closely spaced dwellings and the hope is that it can guide local government and Non-Governmental Organizations in future decision making. Three meters spacing between dwellings, however, may not be pos-

* Correspondence should be addressed to: A. Cicione, E-mail: acicione@sun.ac.za; R. S. Walls, E-mail: rwalls@sun.ac.za; D. Rush, E-mail: d.rush@ed.ac.uk

sible due to the socio-cultural-political-economic issues associated with informal settlements. This is one of the first papers to demonstrate FDS models against full-scale ISD experiments.

Keywords: Informal settlements, Computational fluid dynamics, Enclosure fire dynamics, Full-scale fire experiments, Two zone modelling

1. Introduction

In the world, there are currently an estimated 300,000 fire-related deaths per year with more than 95% of those deaths occurring in middle to lower-income groups [1]. The rapid population growth in cities that is being observed more acutely in the global south, has the potential for more people to reside in informal settlements. An informal settlement refers to dwellings (mostly informal dwellings) erected on land that has not been proclaimed as residential [2]. Informal settlements are also known by other names such as slums, squatter camps or shantytowns in other parts of the world. Informal settlement dwellings (ISDs) are makeshift structures that are typically cladded with immediately available building materials like steel sheeting, plastic sheets or timber; insulated with timber or cardboard; and are often constructed with timber frames. Figure 1 provides an overview of a typical ISD with details pertaining to construction practices and considerations needed for numerical modelling. The details given in Fig. 1 are based on the authors' visits to informal settlements, interviews conducted with firefighters in South Africa by the authors and the literature [3–5]. Therefore, people residing in informal settlements are vulnerable to fire since these areas can be characterized by poorly constructed dwellings, a lack of basic services and are more densely populated than formal settlements [6].

The number of people that reside in informal settlements is expected to increase from one billion worldwide to 1.2 billion people in Africa alone by 2050 [6]. It is of concern, therefore, to see how little work is being done to improve the fire safety in these communities. There are numerous fire incidents illustrating the scale of the problem. For example, In Nepal, 38,924 homes were destroyed by fire incidences between 1990 and 1996 [7]. In January 2005, February 2008 and March 2009 more than 3600 homes were destroyed, leaving more than 13,000 people homeless in the Joe Slovo informal settlement in Cape Town [8]. In May 2012 a fire ravaged an informal settlement in Accra, Ghana, leaving approximately 3500 people homeless [9]. In April 2014, in Valparaíso, approximately 2500 homes were destroyed by a fire, leaving 12,500 people homeless [10]. In 2017, approximately 2200 homes were razed, affecting approximately 9700 people in the Imizamo Yethu informal settlement in Cape Town [11]. These fires do not just cause loss of life in these communities, but significant morbidity with over 10 M disability adjusted life years lost each year due to fire, and loss of belongings (such as official documents, educational material) and livelihoods.

The development and validation of Computational Fluid Dynamics (CFD) models in the fire community has so far generally focused on small-scale fire behaviour and smoke movement [12–15] with some validations of post-flashover com-

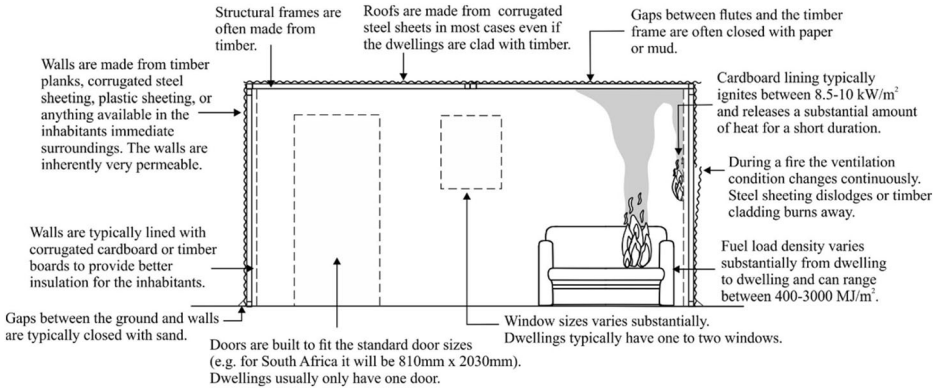

Figure 1. Typical informal settlement dwelling with details needed to understand the fire dynamic behaviour of the dwelling.

partment fires [12, 16–18]. All of these studies are based on formal structures (i.e. dwellings with no wall permeability, thick walls, typically not lined with flammable materials, no structural collapse, etc.) and there is negligible literature available on CFD modelling for ISDs. It is with this backdrop that this paper seeks to (a) demonstrate different numerical modelling techniques by comparing the modelling results to full-scale ISD burn experimental results, (b) to provide an understanding of the fire behaviour of ISDs as well as the effect of different cladding materials (i.e. corrugated steel cladding vs. timber cladding) and (c) to provide a Fire Dynamics Simulator (FDS) based solution to evaluate the critical separation distance between dwellings. This work forms part of an overall project to understand fire behaviour in informal settlements. Previous work has focused on results from preliminary single dwellings experiments [5], results from multi-dwelling experiments considering inter-dwelling spread [19], the development of a simplified FDS model to describe the aforementioned multi-dwelling experiment [20], analysis of large-scale spread in a real fire disaster that affected over 2000 homes [11], and the appraisal of fire safety interventions to be used in such settlements [21].

2. Experimental Set-Up

Two full-scale ISD fire experiments were conducted at the Breede Valley Fire Department in Worcester, South Africa; namely (a) a corrugated steel sheeting clad experiment and (b) a timber clad experiment. The thermocouples used were K-Type thermocouples and the Thin Skin Calorimeters (TSCs) used were constructed according to [14] and have an accuracy of $\pm$ 10% and a measuring range of approximately 0–200 kW/m^2. The TSCs used in the experiments were validated and calibrated against a water-cooled heat flux gauge. The timber fuel (i.e. Pine) used had a density of 536 kg/m^3 with a gross heat of combustion of 18 MJ/kg, the cardboard used had an approximate thickness of 1.5 mm with a density of approximately 180 kg/m^3 and a gross heat of combustion of 16.9 MJ/kg. The

gross heat of combustion of the timber and cardboard were measured with a bomb calorimeter. For both experiments, the roofs were made from corrugated steel sheeting with a thickness of 0.47 mm and the frames of both experiments were constructed from 50 mm × 50 mm timber sections (i.e. Pine). The timber clad dwelling was cladded with 12 × 100 mm (thickness × width) timber planks. The corrugated steel sheeting dwelling was cladded with 0.47 mm thick sheeting with a flute height of 17 mm. Figure 2 depicts the details pertaining to the two experiments. All the equipment was not present in each experiment, after the first experiment (i.e. the steel clad dwelling experiment) and the analysis of the data, the equipment layout was adjusted based upon the authors' observations and findings. It was decided that an equipment tree at 1 m away from the window should be added for the timber clad dwelling experiment. This was decided to ensure that more data could be collected at a distance, which is important when considering fire spread.

Note that all TSCs were orientated at the dwelling, with the direction parallel to the ground, facing into the door or window. The only difference between the two experiments was the cladding material of the walls. Figure 3 visually depicts the steel clad dwelling and timber clad dwelling.

2.1. Fuel Load

In 2015, a survey was conducted in an informal settlement through the University of Stellenbosch, where it was found that the average fire load density was 410 MJ/m^2 with a standard deviation of 140 MJ/m^2 [22]. However, the sample size was too small to be considered fully reliable. In 2017, interviews were conducted at the Breede Valley Fire Department by the authors. The firefighters that were interviewed fought more than 2000 informal settlement fires incidents combined. According to them, the average fire load density in an ISD is higher than formal dwellings (i.e. probably higher than 780 MJ/m^2 as stipulated in EN 1991-1-2 (CEN 2009)). In some cases, the fire load densities can be as high as 1000–2000 MJ/m^2 depending on the occupation of the resident of the dwelling (e.g. inhabitants storing paraffin, wood or tyres) [4, 5]. The fire load densities vary substantially from settlement to settlement as a result of the building materials available in the immediate surroundings of a particular settlement and also as a result of variation in income levels. In this work it was decided to use the average fire load density of 780 MJ/m^2 as specified by [9] for formal dwellings. In order to mimic reality, cardboard insulation was added to the inside of the walls of the dwelling as one would typically find in these dwellings. Additionally, polystyrene was added to the wood cribs to increase the fire spread rate, although during the experiment it was noted that the polystyrene had a negligible effect on the spread rate, and it is not recommended for future work. The wood cribs and cardboard insulation are depicted in Fig. 4. There were 36 timber pieces (40 × 60 × 900 mm) per crib and the crib configuration is also shown Fig. 4.

The dwellings were ignited by igniting a tin can (100 mm in diameter and 200 mm high) filled with approximately 1.5 L paraffin (kerosene). The tin can was placed in the middle front crib (i.e. crib 2 as depicted in Fig. 2). For the steel clad

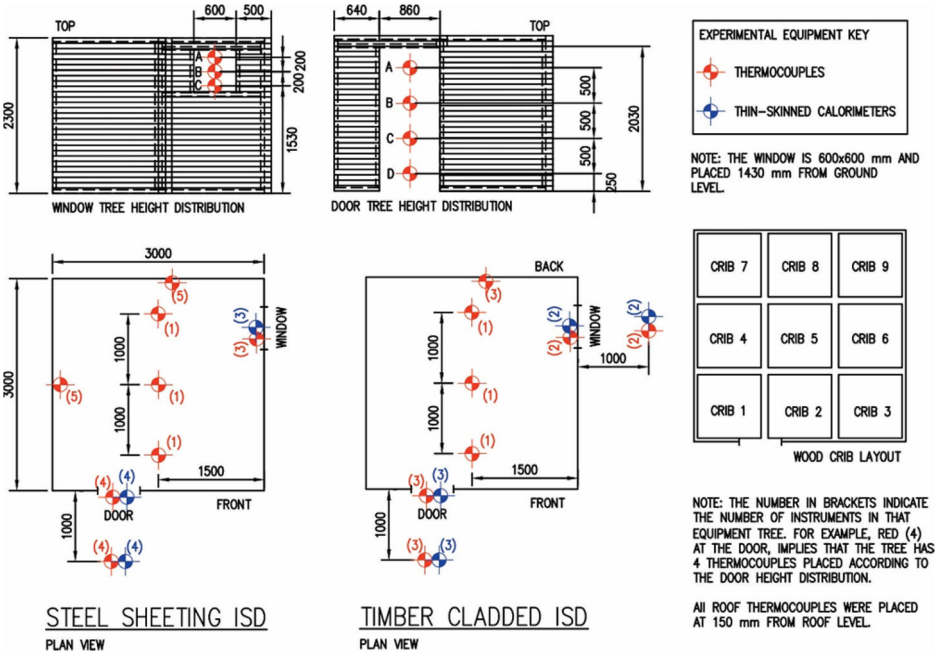

Figure 2. Experimental setup: Floor plans with experimental layout are depicted by the bottom left layouts and the height distributions of window trees and door trees are depicted by the top left layouts. All trees, not placed in front of a door or window, were distributed according to the door tree height distribution, unless stated otherwise.

Figure 3. Steel clad dwelling setup (left image) and timber clad dwelling setup (right image).

experiment, two timber pieces placed at the top of crib 2, above the can, were partially dipped (i.e. approximately 200 mm of the tip of the timber piece) in paraffin to increase the initial growth phase. However, the fire brigade did allow

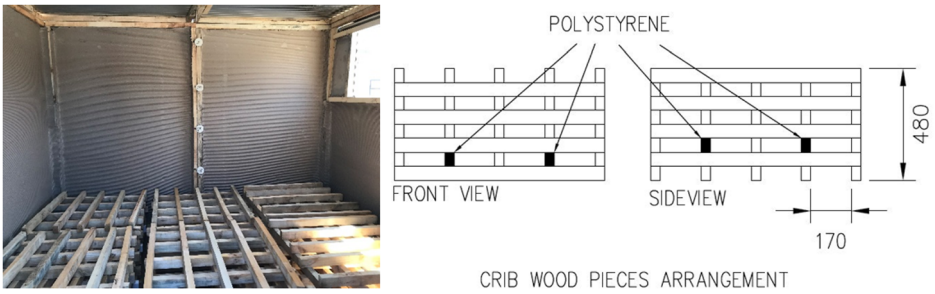

Figure 4. Fuel load for both steel sheeting clad ISD and timber clad ISD experiments (Note that all dimensions are in mm).

some of the paraffin to drip on the crib as they placed the timber pieces back in position. After the first experiment (i.e. the steel clad experiment) it was decided to increase (double) the number of timber pieces dipped in paraffin to increase the initial growth phase.

3. Experimental Results

3.1. Corrugated Steel Sheeting Clad ISD Results

As introduced above, the corrugated steel clad experiment was conducted at the Breede Valley Fire Department in Worcester, South Africa. The ambient temperature was 29°C and a very light North Westerly breeze (i.e. from the front left to the back right of the test setup as depicted in Fig. 2), with wind speeds fluctuating between being negligible and 2 m/s, based on the local wind readings. Approximately 11 min after the paraffin source was ignited, the flames had grown high enough to just reach the cardboard lining, at this point the cardboard on the front wall caught fire and flashover ensued approximately 12 s later. Flashover in this paper refers to the transition phase between the growth stage and the fully developed fire stage. The fire in the compartment attained a fully developed state seconds after flashover was reached. The flames could be seen emerging out of the door and the window. Flames from the door and window of 3–4 m high, from ground level, were recorded. Figures 5 and 6 depict the experimental ceiling and back wall temperatures, respectively. The thermocouple (TC) heights shown in Fig. 6 are from ground level. Note that the height distributions of instruments placed (a) in front of the door, (b) in front of the window or (c) at ceiling level, are presented in Fig. 2. Due to the intensity of the fire and because of structural collapse, a number of the thermocouples and Thin Skin Calorimeters (TSCs) got damaged during the experiments. Thus, if a measurement at certain instrument position is not portrayed, it can be assumed that the instrument was damaged at that particular position.

It is important to note that structural collapse occurred at approximately 19 min and that no data is considered after collapse for the rest of the discussion that follows. The temperatures across the ceiling were relatively uniform with an

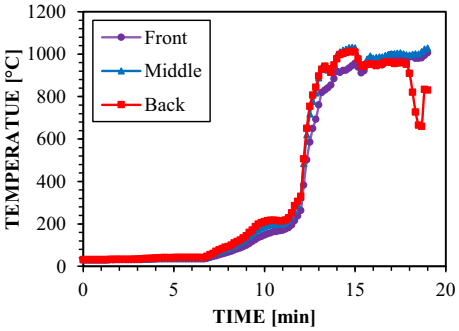

Figure 5. Experimental ceiling temperatures.

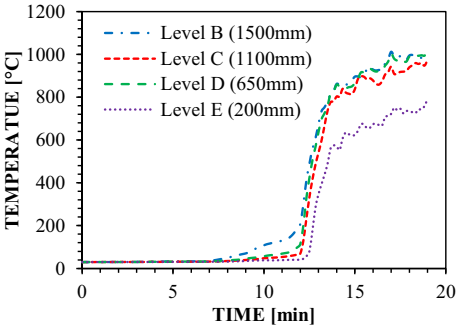

Figure 6. Experimental back wall temperatures.

average steady state temperature of 1000°C and a maximum temperature of 1032°C, as depicted in Fig. 5. It is also clear that this dwelling was ventilation controlled once the fully developed stage was reached as indicated by the plateau in Fig. 5. After flashover the temperatures over the height of the compartment were relatively uniform, as depicted in Fig. 6, with the only cooler part being at the bottom of the timber cribs. Figures 7, 8 and 9 depict the heat flux curves at the door, at 1 m away from the door and at the window, respectively.

The heat flux at the door reached a maximum of 213 kW/m^2, which is beyond the calibration limits and should be interpreted accordingly. This peak corresponds with the complete ignition of the cardboard lining. The average steady state heat flux at the door (Level A) was 88 kW/m^2, as depicted in Fig. 7. The average steady state heat flux at the window (Level A) of 80 kW/m^2 is relatively similar to the heat fluxes experienced at the door. However, the maximum of 132 kW/m^2 is less than the peak experienced at the door. The heat flux curves at the window show no peak that corresponds with the complete ignition of the cardboard. The average steady state heat flux at 1 m away from the door (Level A) was 32 kW/m^2. The heat fluxes experienced in this experiment are extremely high when considering the Critical Heat Flux (CHF) of cardboard of 8–10 kW/m^2 [23, 24] (i.e. a common lining material used in ISDs). The cardboard of an adja-

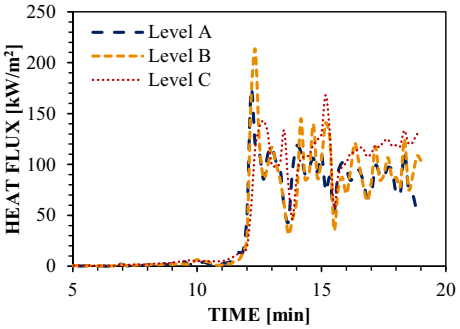

Figure 7. Heat flux curves at the door.

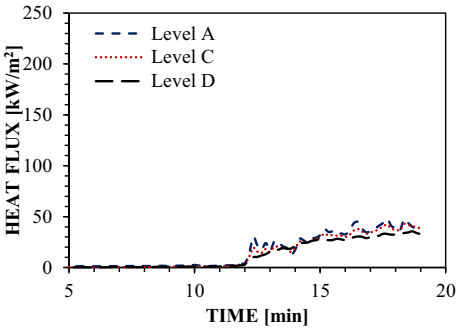

Figure 8. Heat flux curve at 1 m away from the door.

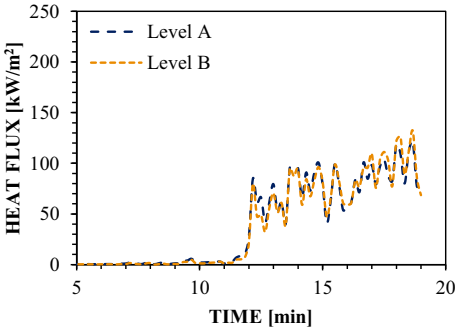

Figure 9. Heat flux curves at the window.

cent dwelling is typically exposed to these heat fluxes as a result of poor construction methods, or gaps as a result of the flutes [19]. This indicates that at 1 m spacing between dwellings, rapid fire spread will occur, highlighting the risk of these closely spaced dwellings.

3.2. Timber Clad ISD Results

The second experiment was also conducted at the Breede Valley Fire Department in Worcester, South Africa, but on a different day. The ambient temperature was 28°C and a very light North Westerly breeze (i.e. from the front left to the back right of the test setup as depicted in Fig. 2), with wind speeds fluctuating between being negligible and 2 m/s. Approximately 3.2 min after the paraffin source was ignited, the flames had grown enough to just reach the cardboard lining, at this point the cardboard on the front wall caught fire and flashover ensued approximately 5 s later. The fire in the compartment attained a fully developed state seconds after flashover was reached. The flames could be seen emerging out of the door and the window. Flames from the door and window of 3–4 m high were recorded. Figures 10 and 11 depict the experimental ceiling and back wall temperatures, respectively. The thermocouple (TC) heights shown in Fig. 11 are from ground level.

It is important to note that structural collapse occurred at approximately 6.4 min and that no data is considered after collapse for the rest of the discussion that follows. The temperatures across the ceiling were relatively uniform with a maximum temperature of 1102°C, as depicted in Fig. 10. This dwelling temperature never reached a steady state as a result of the burning of timber cladding. After flashover was reached the timber cladding ignited and contributed significantly to the total heat release rate. The peak temperature corresponds with the complete ignition of the top timber cladding, as depicted in the top left images in Fig. 12. During the fully developed stage the controlling factor quickly changed from ventilation controlled to fuel control as the timber cladding started to burn away at approximately 4.6 min. This is clearly demonstrated by the sudden drop in heat flux as depicted in Figs. 13, 14, 15 and 16 and is visually depicted in Fig. 12. The experimental ceiling temperature was, however, not affected by the large openings arising as a result of the cladding burning away. This might be as a result of the heat from the burning cribs directly underneath the thermocouple, as shown in Fig. 12 (note that the images are approximately 10 s apart).

Figures 13, 14, 15 and 16 depict the heat flux curves at door, at 1 m away from the door, at the window and at 1 m away from the window, respectively.

The heat flux at the door reached a maximum of 106 kW/m^2. Because this dwelling did not reach a steady state, the average heat flux values during the fully developed fire stage were considered. The average fully developed heat flux at the door (Level B) was 93 kW/m^2, as depicted in Fig. 13. The average fully developed stage heat flux at the window (Level A) of 88 kW/m^2 is relatively similar to the heat fluxes experienced at the door. The average fully developed stage heat flux at 1 m away from the door (Level A) and window (Level A) was 43 kW/m^2 and 50 kW/m^2, respectively.

3.3. Steel Clad Experiment Versus Timber Clad Experiment

Table 1 provides a summary of important parameters pertaining to both experiments such as maximum ceiling temperatures, collapse times and heat fluxes, with details being discussed in the section that follows. Data readings after structural

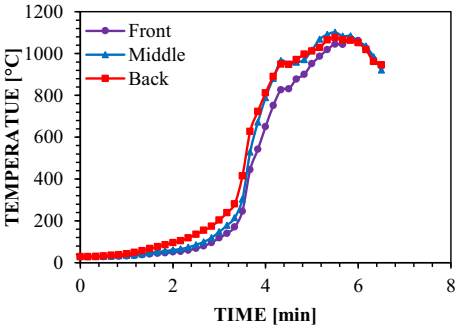

Figure 10. Experimental ceiling temperatures.

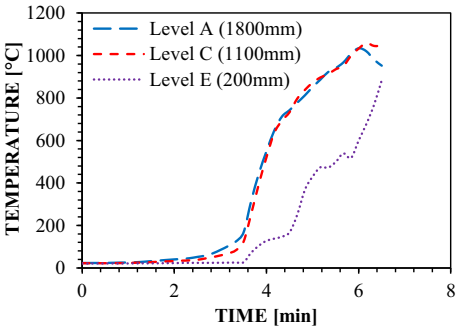

Figure 11. Experimental back wall temperatures.

Figure 12. Ventilation openings forming in the timber clad dwelling experiment as a result of the cladding burning away, showing images at approximately 10 s intervals.

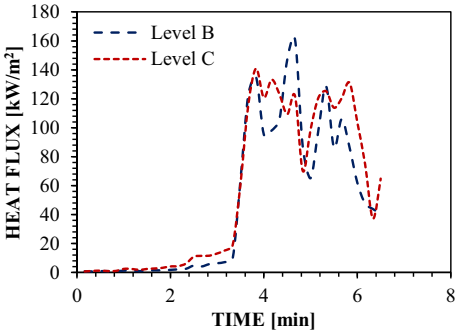

Figure 13. Heat flux curves at the door.

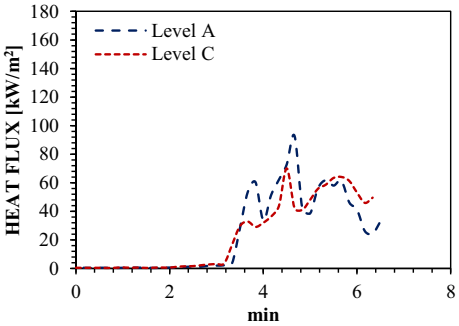

Figure 14. Heat flux curves at 1 m away from the door.

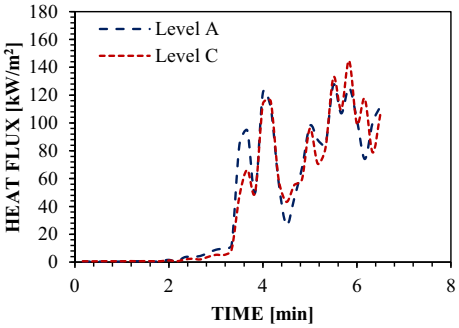

Figure 15. Heat flux curves at the window.

collapse were not considered. Note that the terminology steel clad dwelling and corrugated steel clad dwelling refer to the same experiment.

As mentioned earlier, the timber clad dwelling had more crib timber pieces partially dipped in paraffin that contributed significantly towards the early fire growth of the timber dwelling. This is clear when comparing the time to flashover of

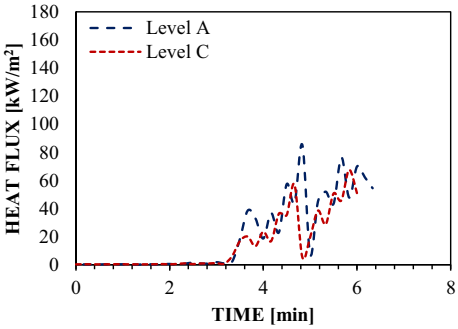

Figure 16. Heat flux curves at 1 m away from the window.

Table 1
A Comparison Between the Corrugated Steel Clad Experiment and the Timber Clad Experiment

	Steel clad experiment	Timber clad experiment
Maximum ceiling temperature	1032°C	1102°C
Time from the start of flashover to collapse	7 min	3.2 min
Heat flux (HF) at the door	95 kW/m^2 (Level B)	93 kW/m^2 (Level B)
HF 1 m away from the door	32 kW/m^2	43 kW/m^2
HF at the window	80 kW/m^2	88 kW/m^2
HF 1 m away from the window	n/a	50 kW/m^2

All heat flux values are the average heat flux value during the fully developed stage obtained at Level A of the specified position unless specified otherwise

7 min for the corrugated steel clad dwelling to the 3.2 min of the timber clad dwelling. Because the timber pieces used for cladding were so thin, it burned away very quickly after it ignited. This left the timber dwelling without lateral support and as a result of eccentricities inherent in the structure the timber dwelling experienced a sway collapse. In general, the heat fluxes experienced during the timber clad experiment were higher than the steel clad experiment, as listed in Table 1, indicating that fire spread to an adjacent dwelling is more likely to occur for the timber dwellings. This is similar to the findings in [19]. The timber dwelling did, however, experience a quicker time to collapse (similar to the findings in [25]), indicating that the heat flux experienced by an adjacent dwelling will be over a shorter period. Additionally, as a result of continuously changing ventilation conditions, the timber clad dwelling had substantial fluctuations in heat flux values, whereas the steel clad dwelling reached a steady state seconds after flashover. Regardless of the factors mentioned above, the average heat flux values for timber dwelling are still enough to ignite adjacent dwellings and are more prone to fire spread than steel dwellings, even if the burning period is only 3 min [19].

4. Fire Dynamic Simulator Model Set-Up

Two FDS models (i.e. a timber clad dwelling model and steel clad dwelling model) were created and the details pertaining to each model are discussed in more detail below.

4.1. Geometry, Computational Domain and Cell Size

The geometry of the dwellings was constructed according to Fig. 2 for both models (the only difference being the cladding material). Both models had a domain size of 5 × 5 × 3 m (i.e. width × breadth × height) with a corresponding cell size of 50 mm^3, giving a total of 600,000 cells. In this case, the timber pieces used in the cribs had a cross sectional area of 60 × 40 mm, which governed the cell size. In order to simplify the cell size ratios, it was decided to model the timber pieces as 50 × 50 mm, thus simplifying the cell size to 50 × 50 × 50 mm, rather than 60 × 40 × 40 mm. Alternatively, a cell size of 20 mm^3 could have been used, however that would have increased the computational time dramatically making it computationally difficult to simulate informal settlement dwelling fires. In order to account for the change in volume of the timber pieces, the density of the timber used for the cribs in the simulations was adjusted to 515 kg/m^3. The same problem occurred for the cardboard. The actual thickness of the cardboard was 1.5 mm, but the cell size of 50 mm would not allow such a thin obstruction. The cardboard was thus modeled as 50 mm thick (i.e. to be at least one cell size thick which allows the obstruction to have full functionality [26]) and the density modified to account for the change in volume of the obstruction. Figure 17 depicts the setup as a Smokeview image [27]. The walls' surface properties (i.e. the HVAC system and the slots between timber layers) are explained in the section that follows. Note that wind was not accounted for in the models and that the domain boundaries were modeled as open.

Unfortunately, as a result of limitations on both the University of Edinburgh and Stellenbosch University's High Performance Computers (HPCs), a cell sensitivity study could not be done. Decreasing the cell size to 25 mm^3, increased the number of cells to 4.8 million. After running the simulation for one month the simulation did still not reach the flashover stage. A model with such a refined mesh is economically unpractical and will make it difficult to use the developed model for parametric studies. Since, the cell size is governed by the thickness of the timber pieces, a bigger cell size could also not be considered for the cell sensitivity study. The cell size used in the models developed in this work is significantly smaller than 0.1D* (i.e. a theoretical value for the maximum cell size for plume fires according to [28]). Where D* can be calculated as follows:

$$D^* = \left(\frac{\dot{Q}}{\rho_\infty T_\infty c_p \sqrt{g}}\right)^{2/5} \tag{1}$$

where D^* is the characteristic length scale of the fire plume, $\dot{Q}$ is the heat release rate [kW], ρ_∞, T_∞ and C_p are the ambient air density [kg/m^3], specific heat of air

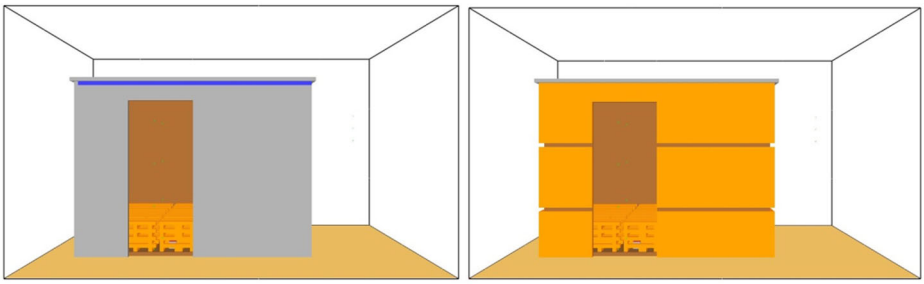

Figure 17. Geometry of the steel clad dwelling (left) and the timber clad dwelling (right) used in the numerical simulation (Smokeview).

[kJ/(kg K)] and ambient temperature [K], respectively and g is the gravitational acceleration [m/s^2]. For $\dot{Q}$ = 10,250 kW (i.e. for the nine cribs in this case, calculated according to Babrauskas's HRR for cribs method [29]), a characteristic fire diameter of D* = 2.4 m is obtained, meaning a minimum cell size of 0.1D* = 0.24 m is required according to [28]. In this work, a cell size of 0.05 m was used, which is significantly smaller than 0.1D*. The 0.1D* method is widely used in the fire community and has shown good results in past studies [30–34]. The method also showed good results for timber crib models [35, 36]. Additionally, the authors conducted a cell sensitivity study in [20], where the model consisted of multiple ISDs with the same (i.e. compared to the current models) cladding materials and cardboard lining and it was found that a cell size of 0.1 m (a cell size of 0.05 m was used in this work) was sufficient to capture the ceiling temperatures, heat fluxes emitted from the dwelling and the cardboard behaviour. Thus, with all of the factors mentioned above, it can be assumed with reasonable certainty that the cell size used in this work is sufficient enough to capture the fire behaviour with reasonable accuracy.

4.2. Material and Surface Properties

Table 2 gives the properties of the materials used in the FDS models. The material properties of the steel, cardboard and wood were taken from [24, 37–41], respectively.

For both the steel clad dwelling and timber clad dwelling model, the timber crib pieces and cardboard both had a prescribed surface thickness of 25 mm applied to all faces, with a void backing condition. To model the timber pieces that were dipped in paraffin an ignition temperature of 30°C was prescribed to start the burning of those pieces immediately. It should be noted that the time to flashover is relatively sensitive to the quantity of timber pieces modelled as dipped in paraffin. Because this was difficult to quantify, the number of timber pieces modelled as dipped were increased to enable the model to reach flashover earlier in order to reduce the computational time of the simulation, thus allowing for multiple scenarios to be studied within a reasonable time (note that a simulation still took 2–

Table 2
Material Properties Used in the FDS Models

Properties	Steel	Corrugated cardboard	Wood
Density [kg/m^3]	7850	180 (actual)—5.4 (used in FDS)	536 (actual), 515 (used in FDS)
Specific Heat [kJ/(kg K)]	0.6	2.7	1.3
Conductivity [W/(m K)]	45	0.42	0.14
Emissivity	0.42 [38] (i.e. for new galvanised steel)	0.9	0.9
Ignition temperature [°C]	n/a	293	350

3 weeks on the HPCs). The results were offset in order for the flashover phases to match.

For the steel sheeting clad dwelling model, the flutes created additional openings (i.e. at wall and roof connections) which are smaller than the cell size but are typical of ISDs. The leakage was modelled in FDS by using HVAC systems, using its 'leak' functionality. The leak area and flow loss were specified as 0.0255 m^2 and 0, respectively for the steel clad model. The steel sheets were modeled as flat sheets with a surface thickness of 0.025 mm applied to all faces and a backing condition of exposed.

For the timber clad dwelling model, the walls were modeled as 50 mm thick to be at least one cell size thick with the density modified to account for the change in volume of the obstruction. A surface thickness of 25 mm was applied to all surfaces with a backing condition of air gap. A horizontal 50 mm gap was specified over the width of all walls at 800 mm and 1500 mm from ground level of the walls, as depicted in Fig. 17. This was to account for the small gaps between each 100 mm cladding timber plank, as seen in the top left image in Fig. 12. The positions of the gaps (i.e. the gaps at 800 mm and 1500 mm) were arbitrarily decided on. The positions of these gaps will affect the ceiling temperatures but will not have a substantial effect on the heat fluxes experienced in front of the door and window.

4.3. Prescribed Heat Release Rate Obtained Through FPA Test

The heat release rate per unit area (HRRPUA) curves for these models were obtained by means of a Fire Propagation Apparatus (FPA) test and are depicted in Fig. 18. The FPA is an apparatus that can be used to quantify the convective, chemical and overall heat release rate, mass loss rate and the effective heat of combustion of a material. For a detailed description of the FPA the reader is refer to [42]. Since the heat flux emitted onto the timber cribs and cardboard are expected to be 50 kW/m^2 or higher, the heat flux used during the FPA test was 50 kW/m^2. According to previous studies (e.g. [35]), the peak HRRPUA output from FPA or cone calorimeter tests are similar for higher heat flux values (e.g.

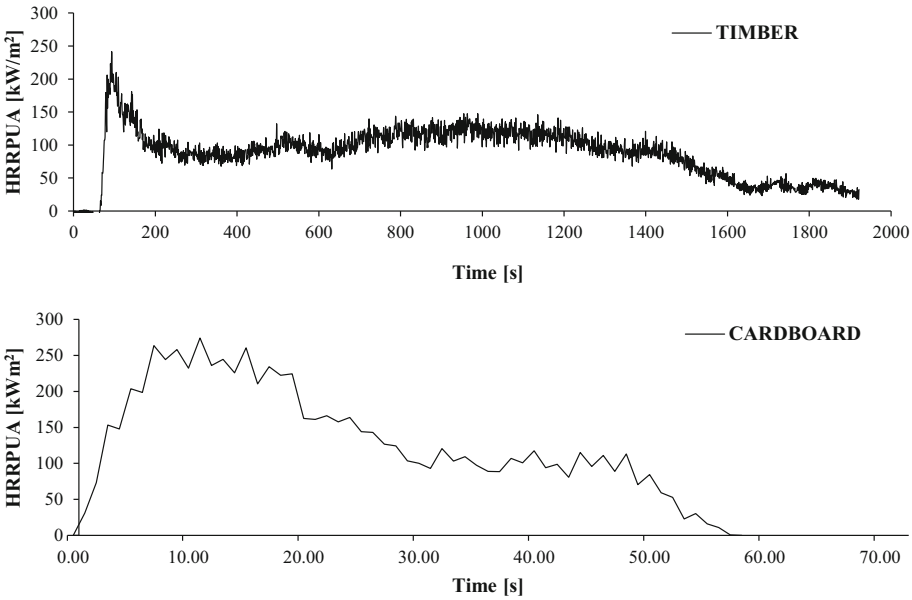

Figure 18. Heat release rate per unit area curve for timber (top graph) and cardboard (bottom graph).

50 kW/m^2 as used in this work). The exact values (i.e. from Fig. 18) were used as an input in FDS to prescribe the HRRPUA of the two fuel materials.

The value of the heat release rate (HRR) of the timber cribs according to the SFPE timber crib calculations by Babrauskas [29] are described by the following very well-known HRR formula:

$$\dot{Q} = \dot{m}\Delta H_{eff} \tag{2}$$

where $\dot{m}$ is the mass loss rate measured in kg/s and ΔH_{eff} is the effective heat of combustion measured in kJ/kg. The mass loss rate, $\dot{m}$, is taken as the lesser of the surface-controlled mass loss rate

$$\dot{m} = \frac{4}{D} m_0 v_p \left(1 - \frac{2 v_p t}{D}\right) \tag{3}$$

and porosity-controlled mass loss rate

$$\dot{m} = 4.4 \times 10^{-4} \left(\frac{S}{h_c}\right) \left(\frac{m_0}{D}\right) \tag{4}$$

For the cribs used in this experiments, the stick thickness was D = 0.04 m, the clear spacing was S = 0.175 m, the crib height was h_c = 0.48 m, the number of sticks per row was n = 5, the initial crib mass was m_0 = 41.67 kg, v_p = 2.2 ×

10^{-6} $D^{-0.6}$ according to [29] and the heat of combustion was ΔH_{eff} = 18 MJ/kg (assuming a combustion efficiency of 1, the effective heat of combustion equals the gross heat of combustion). This gave an experimental surface-controlled mass loss rate with a limiting HRR of 1138.37 kW.

In the modelling, to simplify the cell size ratio and reduce the computational time the stick thickness was changed to D = 0.05 m as discussed above, the clear spacing to S = 0.1625 m and the crib height to h_c = 0.4 m. Using Eqs. 2–4 the modelling HRR would be 769.57 kW. Thus, by using a cross sectional area of 50 × 50 mm rather than 60 × 40 mm leads to a 32% decrease in the HRR of the cribs according to Babrauskas' formulas. To account for this within the model, the heat of combustion on the material line (i.e. in FDS) was increased by 32%, giving a heat of combustion of 23.8 MJ/kg, to obtain the same HRR one would expect for the experimental timber cribs. The reaction line for both models looked as follows: &REAC ID = 'WOOD', FUEL = 'REAC_FUEL', C = 3.4, H = 6.2, O = 2.5, SOOT_H_FRACTION = 0.0, SOOT_YIELD = 0.03, HEAT_OF_COMBUSTION = 1.8E4/. The simple chemical composition and soot yield values used on the reaction line (in FDS) were obtained from [43, 44].

5. Two-Zone Model Set-Up

It would be advantageous for the development of interventions for ISD fire safety if simple two zone models could be used to quickly obtain estimates of fire behaviour, rather than a CFD model being utilized each time. This also would allow parametric and statistical analyses to be carried out more easily. Hence, OZone v3 [45] was also used to model both the steel clad and timber clad ISD experiments. OZone is a one and two zonal fire modelling software designed by the University of Liège in Belgium. During the duration of a fire, the temperature development of gases inside the enclosure are evaluated by zone models. The compartment under consideration is divided into zones and the main hypothesis made is that the temperature distribution is uniform in each zone at any time. The temperature, species concentration and size of each zone are calculated with a dynamic process as the fire progresses, together with the smoke movement through openings in the compartment boundaries, by applying the moment, mass and energy conservation laws to each zone. Since, zone models cannot calculate fire spread it requires certain inputs such as the fire growth rate. For OZone outputs typically include the zone height and gas temperatures. For more information regarding the formulations of OZone, the reader is referred to [45]. In general, the OZone default values were used. The user is able to choose between four air entrainment models in OZone and the following should be considered:

- McCaffrey [46]: This air entrained model considers the all the regions (i.e. plume region, flame region and the intermittent region).
- Heskestad [47]: This air entrained model considers only the plume region and the flame region and does not consider the intermittent region as in [46]. This is

the default air entrained model in OZone and is implicitly used in the manual calculation method.
- Thomas [48]: This air entrained model is best suited for use in the vicinity of a flame region.
- Zukoski [49]: This air entrained model is theoretically only suitable for the plume region and the use of this model is questionable for zone models with low ceilings (e.g. for ISDs).

Since there is insufficient space for a complete plume to develop above the fire region and because the fire region will extend across the entire enclosure the air entrained models which consider the flame and intermittent regions (i.e. [46]) will describe the air entrainment best. It was decided to use the McCaffrey model [46] in this work.

For the steel dwelling model, a HRRPUA of 1138.37 kW/m^2, a fire growth rate of 233.8 s and a fire load density of 750.23 MJ/m^2 (i.e. the timber cribs fire load density) plus 17.5 MJ/m^2 (i.e. cardboard lining fire load density) were specified. The heat release rate of 10,245.31 kW was calculated according to the SPFE HRR wood crib calculations by Babrauskas [29], where the stick thickness is 0.04 m, the clear spacing is 0.175 m, the crib height is 0.48 m, number of sticks per row is 15, initial crib weight is 375.03 kg and the heat of combustion is 18 MJ/kg. To convert the HRR to a HRRPUA the floor area of 9 m^2 was used to obtain the 1138.37 kW/m^2 value as seen above. It should be noted that OZone does not have the capability to simulate fire spread and thus it is necessary to include a growth rate in the model, although for it, and other methods, analytical methods could be used to provide predicted heat fluxes. The fire growth rate was obtained through a t-squared fire calculation and by setting the fire intensity coefficient equal to 'ultrafast' (i.e. 1.874×10^{-5}). Although wood cribs on their own are better prescribed by a 'fast' fire intensity coefficient (e.g. [50]), 'ultrafast' was used to account for the cardboard lining. The walls were defined as one layer set to Steel [EN1994-1-2] with a thickness of 0.047 mm. The roof and floor were set to Steel [EN1994-1-2] with a thickness of 0.047 mm and concrete with a thickness of 200 mm, respectively. Due to construction tolerances and steel sheeting profiles wall–wall and wall-roof connections were modeled with an 8.5 mm gap. Both the window and door were modeled as open.

For the timber dwelling model, a HRRPUA of 1138.37 kW/m^2, a fire growth rate of 233.8 s and a fire load density of 750.23 MJ/m^2 (i.e. the timber cribs fire load density) plus 17.5 MJ/m^2 (i.e. cardboard lining fire load density) plus 546.6 MJ/m^2 (i.e. timber cladding fire load density) were specified. The roof and floor had the same input parameters as for the corrugated steel clad dwelling model. The walls were set to timber with a 12 mm thickness, 536 kg/m^3 density, 0.14 W/(m K) conductivity, 1300 J/(kg K) specific heat and an emissivity of 0.9 (see Table 3). Due to the construction configuration the wall–wall and wall-roof connections were modeled with an 8.5 mm gap. OZone is limited to 3 openings per wall and thus a small gap between each timber plank (i.e. the timber cladding) is not able to be modeled and to account for this the wall-roof connection gap was increased from 8.5 mm to 100 mm (i.e. to account for all the small gaps

Table 3
Summary of Selected Data from (a) Experimental Results, (b) FDS Model Results and (c) Two-Zone Model Results

	Experiment	FDS model	Two-zone model
Maximum ceiling temperature	1032°C	985°C	1085°C
Time from the start of flashover to collapse	7 min	n/a	n/a
Heat flux (HF) at the door	88 kW/m^2	105 kW/m^2	n/a
HF 1 m away from the door	32 kW/m^2	34 kW/m^2	n/a
HF at the window	80 kW/m^2	84 kW/m^2	n/a

All heat flux values are the average steady state heat flux value obtained at Level A of the specified position. Note that where steady state was not reached, the average heat flux during the fully developed stage was used

between the timber cladding, similarly to what was done in the FDS model). Both the window and door were modeled as open.

6. Numerical Modelling Results and Comparison

This section is divided into two subsections; (a) the corrugated steel sheeting clad model results and comparison and (b) the timber clad model results and comparison.

6.1. Corrugated Steel Sheeting Clad Results and Comparison

Table 3 provides a summary of important parameters pertaining to the experiment, the FDS model and the two-zone model such as maximum ceiling temperatures, collapse times and heat fluxes (HF), with details being discussed in the sections that follow. Data readings after structural collapse were not considered.

The ceiling time–temperature curve of the FDS model, two zone model and the experimental results are depicted in Fig. 19. The ceiling temperatures for the experimental results were measured in the middle of the dwelling and are referred to as the experimental TC results in Fig. 19.

The initial growth phase of a fire cannot be modeled in OZone (one of the limitations of two-zone modelling), so the two-zone model results were offset by 7.8 min for the flashover stages of the model and experiment to align. The two-zone model compares well to the experiment (considering the simple nature of the model), with the plateau following the correct trend and the temperatures reached have a maximum deviation of approximately 8% during the fully developed fire stage. The FDS model captures the behaviour of the cardboard lining quite well. From the temperature slice files, it is clear that flashover occurred as a result of radiation from the flames of the burning cardboard, as depicted in Fig. 20, similar to what was observed during the experiments. This is clear when considering the hot layer build up before the cardboard ignites, and then considering the hot layer during the burning of cardboard. The radiation from the hot layer did still contribute towards the ignition of the cribs, but in a less substantial way in compar-

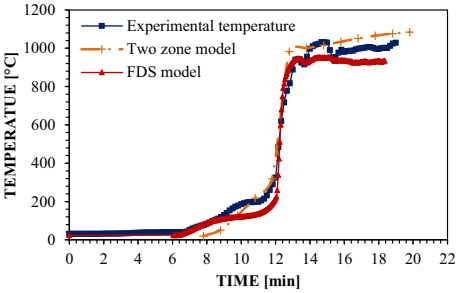

Figure 19. Ceiling temperatures for the corrugated steel clad ISD.

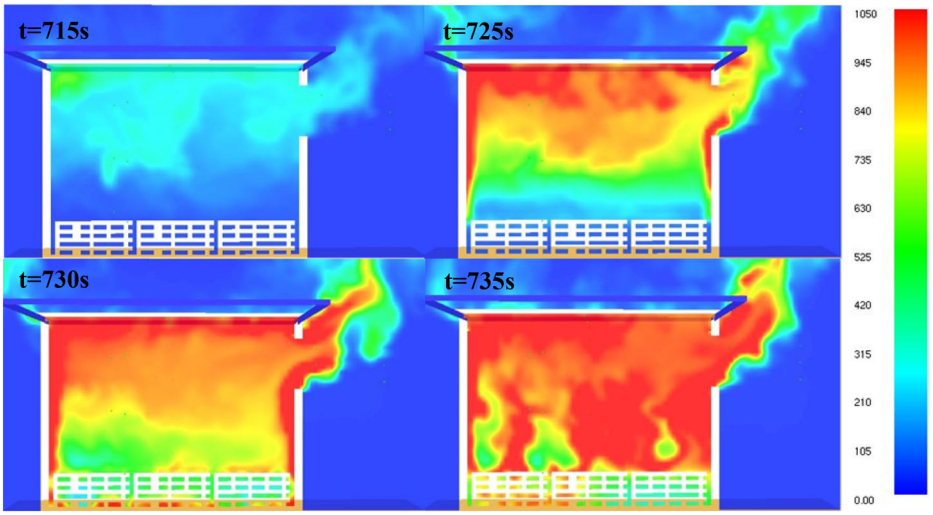

Figure 20. Temperature slice file from FDS at the window for the steel clad dwelling, showing the heat emitted from the cardboard lining.

ison to the radiation from the cardboard, similar to the findings in [19]. The ceiling temperatures predicted by the FDS model are slightly underpredicted, but the general trend compares well to the experiment i.e. when considering the growth stage, flashover, and the trend of the plateaus. The FDS model has a slightly steeper slope during the flashover stage; this is as a result of the approximate cardboard properties used in FDS (e.g. using a slightly higher ignition temperature will result in slower fire spread across the surface of the cardboard, and as a result it causes flashover to happen less rapidly, the conduction, specific heat and density of the cardboard can also affect this behaviour). Comparing the surface spread rate of the cardboard in the model to the experimental surface spread rate, it is clear that the fire spreads faster in the model. From the experimental results it is

clear that this dwelling was ventilation controlled and it is also portrayed by the two-zone and FDS models.

The heat flux curves at the door and at 1 m away from the door of the FDS model and the experimental results are depicted in Figs. 21 and 22, respectively. OZone models do not have the capability to predict heat flux values and are thus not discussed further in this section. This is another limitation of two-zone models. Heat fluxes are an extremely important parameter when studying fire spread and the intensity of the fire.

The heat fluxes at the door of the FDS model compare relatively well to the experimental values, as depicted in Fig. 21. Considering the heat flux curve at Level A and B of the FDS model and of the experiment, it is clear that the overall trend is captured by FDS. Although the peak heat flux values at approximately 12 min (i.e. where the cardboard was completely engulfed with flames) are lower for the FDS model, the model does capture the behaviour of the peak corresponding to this complete ignition of the cardboard lining well. Although the model underpredicted the peak corresponding to the burning of the cardboard at the door, the model overpredicted this same peak at 1 m away from the door (Fig. 22) and also at the window (Fig. 23). The average steady state heat flux of the FDS model at the door is 105 kW/m^2 which is 19% higher that the experimental average steady state heat flux of 88 kW/m^2. The average heat flux during the steady state stage, at 1 m away from the door, for the model is 34 kW/m^2 which compares very well to the experimental average heat flux during the fully developed fire stage of 32 kW/m^2. Although there are some deviations between the two curves, the overall trend is capture relatively well by the model. The slight deviations might be as a result of (a) the light breeze/wind not being included in the simulation, (b) the assumptions made to model the cardboard lining (i.e. allowing the cardboard to be one cell size thick, and a result reducing the density as explained above), or (c) assumptions made to simplify the timber cribs.

The heat flux curve at the window for the FDS model and the experimental results are depicted in Fig. 23.

The average steady state heat flux at the widow of the FDS model is 84 kW/m^2 and compares well to the experimental value of 80 kW/m^2, as depicted in Fig. 23. Considering the heat flux curve at Level A and B of the FDS model and of the experiment, it is clear that the overall trend is captured well by FDS. The experimental results do not show a peak value at approximately 12 min, whereas the FDS model does.

6.2. Timber Clad Model Results and Comparison

Table 4 provides a summary of important parameters pertaining to the experiment, the FDS model and the two-zone model such as maximum ceiling temperatures, collapse times and heat fluxes, with details being discussed in the sections that follow. Data readings after structural collapse were not considered.

It is difficult to define a steady state heat flux for the timber experiment because the ventilation conditions changed continuously. Thus, it was decided to use the

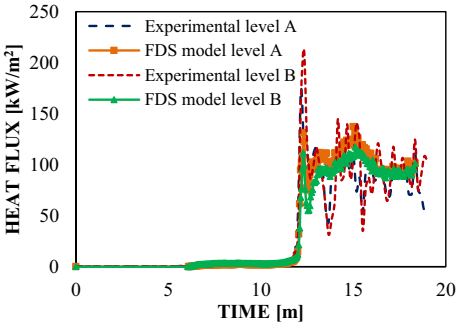

Figure 21. Heat fluxes at the door.

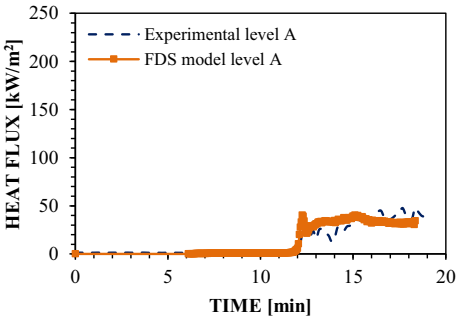

Figure 22. Heat fluxes at 1 m away from the door.

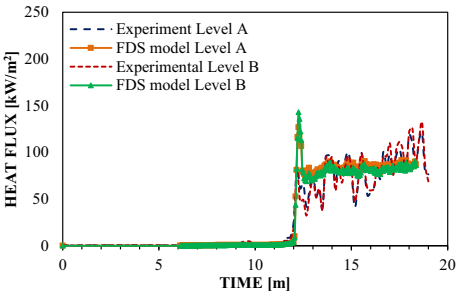

Figure 23. Heat fluxes at the window.

average heat flux during the fully developed stage in order to compare the model results to the experiment results.

The ceiling time–temperature curve of the FDS model, two zone model and the experimental results are depicted in Fig. 24.

The two-zone model slightly overpredicted the ceiling temperature, as compared to the experimental temperatures. The predicted temperatures have a maximum deviation of 25%. This overprediction is likely a result of how the leakages were

Table 4
Summary of Data from Experimental Results, FDS Model Results and Two-Zone Model Results

	Experiment	FDS model	Two-zone model
Maximum ceiling temperature	1102°C	1161°C	1189°C
Time from the start of flashover to collapse	3.2 min	n/a	n/a
Heat flux (HF) at the door	93 kW/m^2 (Level B)	111 kW/m^2 (Level B)	n/a
HF 1 m away from the door	43 kW/m^2	51 kW/m^2	n/a
HF at the window	88 kW/m^2	108 kW/m^2	n/a
HF 1 m away from the window	50 kW/m^2	49 kW/m^2	n/a

All heat flux values are the average heat flux value during the fully developed stage obtained at Level A of the specified position unless specified otherwise

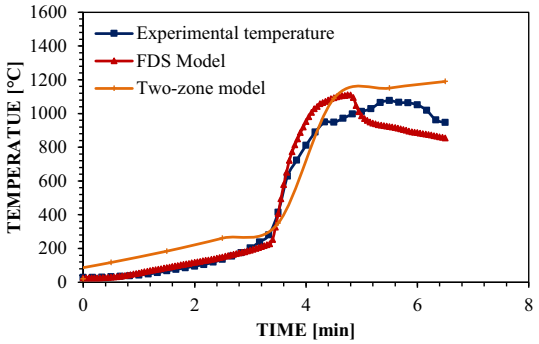

Figure 24. Ceiling temperatures for the timber clad ISD experiment.

modelled in OZone. As mentioned earlier, OZone is limited to 3 openings per wall, thus multiple small openings between timber cladding pieces could not be modelled accurately. The FDS model captures the behaviour of the cardboard lining quite well (similar to the steel clad dwelling). Flashover starts at approximately the same ceiling temperature (i.e. both ceiling temperature approximately at 280°C). The FDS model initially overpredicts the initial ceiling temperature, reaching approximately the same temperatures as the two-zone model. This is likely as a result of the steeper curve during flashover. As mentioned earlier, this is because FDS slightly overpredicts the spread rate across the surface of the cardboard. At 4.9 min the bottom 2/3rds of all the walls were set to instantaneously disappear, in the FDS model, to account for the cladding burning away in the experiment. This could have also been done with a ramp function, or by selecting specific sections to disappear at specific times. However, with all the unknowns such as: which wall started to burn away first, what was the rate at which the walls burned away and where in the wall the gaps first appear, it was arbitrarily

decided (i.e. for simplicity and practicality) to allow the same sections of all the walls to disappear at the same time. Because of this sudden change in ventilation, the FDS ceiling temperatures experienced a sudden dip, rather than a gradual decrease as observe in the experimental results. However, this sudden dip allows the model to capture the heat flux behaviour better and was thus decided to keep to this method of modelling the cladding. The modelling of this complex phenomena will remain a challenge in future work.

The heat flux curves at the door and at 1 m away from the door of the FDS model and the experimental results are depicted in Figs. 25 and 26, respectively.

The heat fluxes at the door of the FDS model compare relatively well to the experimental values, as depicted in Fig. 25. Considering the heat flux curve at Level B and C (Level A was damaged) of the FDS model and of the experiment, it is clear that the overall trend is captured by FDS. The model also captured the peak corresponding to the complete ignition of the cardboard, but overpredicts the peak corresponding with the complete ignition of the timber cladding (i.e. at approximately 4.8 min). The average heat flux during the fully developed stage (i.e. from the end of flashover to collapse) of the model (Level B) is 111 kW/m^2 which is higher than the average heat flux during the fully developed stage of 93 kW/m^2 for the experiment (Level B). It should be noted that the assumptions made to model the timber cladding will have an influence on the results. As depicted in Fig. 26, the curve predicted by FDS captures the experimental curve well with an average heat flux during the fully developed fire stage of 51 kW/m^2 compared to 43 kW/m^2. The overall trend at 1 m away from the door is well captured by the FDS model. In both cases (i.e. at the door and at 1 m away from the door) the model tends to overpredict the heat flux values (especially at the door). As discussed earlier the sudden drop in heat flux at approximately 4.9 min corresponds with the burnout of the timber cladding.

The heat flux curve at the window and at 1 m away from the window for the FDS model and the experimental results are depicted in Figs. 27 and 28, respectively.

Considering Fig. 27 closely, it seems that the FDS model is overpredicting the heat fluxes experienced. In the experiment, the timber cladding at the window started to burn away a lot earlier that the prescribed time in FDS. This is because the sudden drop in heat flux in the experimental results, corresponding with the burnout of the cladding, occurred at approximately 4.3 min, rather than at 4.9 min as modelled in FDS. Additionally, the FDS model overpredicts the peak in heat flux that corresponds with the full ignition of the cardboard. This is mainly due to the following reasons: (a) the assumed combustion efficiency of 1 may be too high (i.e. the heat of combustion of the cardboard could be slightly less), and (b) the way FDS modelled the flame spread across the surface of the cardboard was possibly more rapid than the experiment, meaning more cardboard burned at a particular place in time. This is most likely as a result of the assumed thermal inertia from the literature. Note that a higher thermal inertia will result in a slower surface spread rate. The average heat flux during the fully developed fire stage at the widow of the FDS model is 108 kW/m^2, which is higher than the experimental average heat flux of 88 kW/m^2. Although significant work is

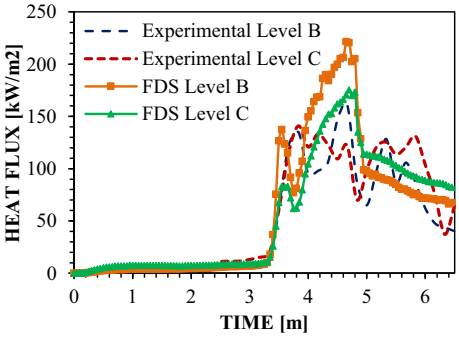

Figure 25. Heat fluxes at the door.

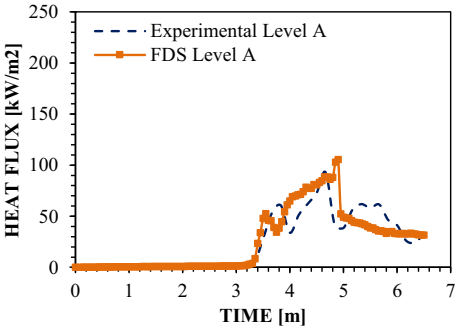

Figure 26. Heat fluxes at 1 m away from the door.

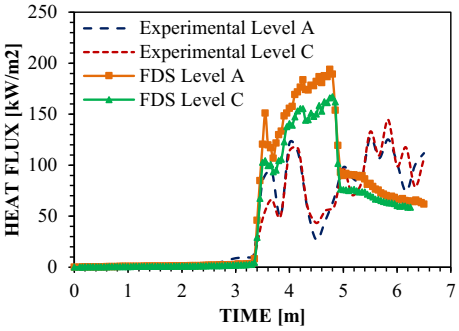

Figure 27. Heat fluxes at the window.

required to refine modelling techniques for timber clad informal dwellings, this work does provide a significant step in the right direction in terms of capturing the general behaviour. Challenges with ventilation conditions varying continuously will not easily be overcome by any modelling software due to the complex input parameters required.

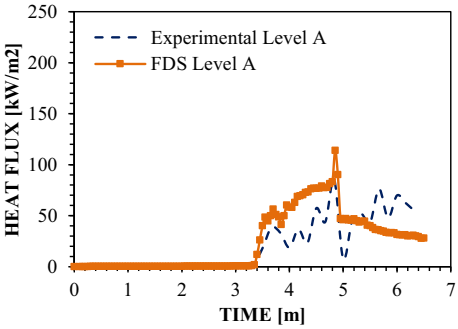

Figure 28. Heat fluxes at 1 m away from the window.

The average heat flux during the fully developed fire stage at 1 m away from the window of the FDS model is 49 kW/m^2, which compares well to experimental average heat flux of 50 kW/m^2. However, if the heat flux values after 4.9 min (i.e. after the timber cladding burned away) are not considered, refer to Fig. 28, the average heat flux of the FDS model would be higher than the experimental value. Although there are some deviations between the two curves, the FDS model does capture the overall trend relatively well.

7. Critical Separation Distance Based on the Numerical Models

Since the FDS modelling techniques employed suitably replicate the experimental results for the steel clad ISD, the model's predictive capabilities can be used estimate a preliminary critical separation distance between ISDs. In order to do this, it is important to quantify the model uncertainty to produce a probability density function (as depicted in Fig. 29) in order to calculate the probability that the model value (i.e. the predicted heat flux) will be exceeded. In other words, it is important to define how accurate the prediction is for a given set of input parameters, and what an anticipated error may be.

To estimate the mean and standard deviation of the distribution the first step is to define $\overline{\ln(M/E)}$ (for a more in depth derivation of the equations that follow, the reader is referred to [51]):

$$\overline{\ln(M/E)} = \frac{1}{n}\sum_{i=0}^{n} \ln(M_i/E_i) \tag{5}$$

where E_i is a given experimental measurement and it is assumed that E_i is normally distributed about the "true" value and that there is no systematic bias. According to [28] this distribution can be assumed because when experimental uncertainties are reported it is typically expressed as a standard deviation or a confidence interval about the measured value. Thus, there is no systematic bias in

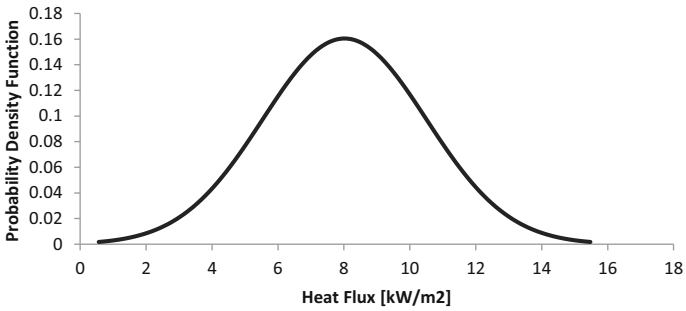

Figure 29. Example of a probability density graph (i.e. a Gaussian Distribution also commonly called a bell curve).

a measured value because it can be quantified and adjusted accordingly. M_i is a given model prediction and it is assumed that M_i is normally distributed about the true values multiplied by a bias factor, δ, (the bias factor is a way to express by what percentage the model is over or under predicting on average, for example, a bias factor of 1.13 means the model is over predicting by 13% on average) and n is the sample size. Peacock et al. [52] discussed various possible metrics with a common metric simply comparing the predicted steady state values. In this work, by comparing the steady state heat fluxes (i.e. comparing the experimental heat fluxes to the modelled heat fluxes) at all the TSC positions, $\overline{\ln(M/E)} = 0.45$ is obtained. Table 5 lists the steady state heat fluxes and TSC positions for both the steel clad dwelling experiment and FDS model along with the procedure used in Eq. 5.

An alternative way of explaining this is by plotting the predicted heat fluxes against the measured heat fluxes, as depicted in Fig. 30. All the horizontal bar and part of the vertical bar represents the total experimental uncertainty [28]. If the experimental uncertainty can be quantified, then the model uncertainty can be obtained as a result.

The least squares estimate of the standard deviation of the combined distribution is defined as:

$$\tilde{\sigma}_M^2 + \tilde{\sigma}_E^2 \approx \frac{1}{n-1}\sum_{i=0}^{n}\left[\ln(M_i/E_i) - \overline{\ln(M/E)}\right]^2 \tag{6}$$

where $\tilde{\sigma}_E$ is the experimental uncertainty, which is known (for heat flux measurements $\tilde{\sigma}_E = 0.11$ [28]), $\tilde{\sigma}_M$ is the model uncertainty. Equation 6 forces a constrained on $\tilde{\sigma}_E$ that the model uncertainty cannot be less than the experimental uncertainty [28] because it is impossible to demonstrate that the model has less uncertainties that the experiment, thus leading to the following expression:

$$\tilde{\sigma}_E^2 < \frac{1}{2}\mathrm{var}(\ln(M/E)) \tag{7}$$

Table 5
Equation 5 Procedure

TSC Position	Experiment result	Model result	In(M/E)
Door (Level A)	89	105	0.17
Door (Level B)	96	98	0.03
Door (Level C)	114	79	− 0.37
1 m from the door (Level A)	33	34	0.04
1 m from the door (Level B)	30	25	− 0.19
1 m from the door (Level C)	26	15	− 0.58
Window (Level A)	80	84	0.05
Window (Level B)	80	81	0.01
			$\overline{\ln(M/E)} = 0.45$

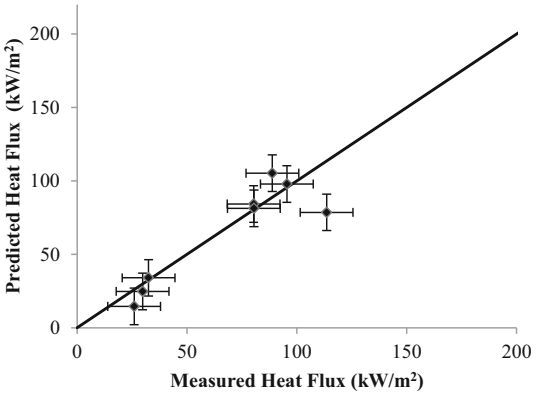

Figure 30. Scatter plot of model predictions and experimental measurements for the steel clad dwelling.

By substituting the known values into Eq. 6, $\tilde{\sigma}_M = 0.23$ is obtained. An estimate of δ can be found using the mean of the distribution:

$$\delta \approx \exp\left(\ln(M/E) + \frac{\tilde{\sigma}_M^2}{2} - \frac{\tilde{\sigma}_E^2}{2}\right) \tag{8}$$

By substituting the known variables into Eq. 8 a bias factor of 0.92 is obtained, indicating that this model tends to underpredict the heat flux values by 8%. From this a mean and a standard deviation can be calculated and from it a bell curve can be drawn:

$$\mu = \frac{M}{\delta} = \frac{5.5}{0.92} = 6; \quad \sigma = \tilde{\sigma}_M \frac{M}{\delta} = 0.23\frac{5.5}{0.92} = 1.37 \tag{9}$$

where M = 5.5 kW/m^2 in this case is the average heat flux, during the steady state phase (starting at approximately 13 min) at 3 m away from the door, predicted by the FDS model. The bell curve is depicted in Fig. 31.

The shaded area beneath the bell curve is the probability that the "true" heat flux can exceed the critical heat flux, and can be expressed via the complimentary error function:

$$P(HF > HF_c) = \frac{1}{2} erfc\left(\frac{HF_c - \mu}{\sigma\sqrt{2}}\right) = \frac{1}{2} erfc\left(\frac{8.5 - 5.9}{1.3\sqrt{2}}\right) = 0.033 \quad (10)$$

This indicates that there is a 3.3% chance that fire spread can occur if the adjacent dwelling is 3 m away, based on these FDS model predictions. Note that a very conservative CHF value for cardboard (8.5 kW/m^2) was used, if the CHF is changed to 10 kW/m^2 the probability of the predicted heat flux exceeding 10 kW/m^2 is 0.16%. Additionally, if the CHF is exceeded the heat flux must be sustained for a specific amount of time for the cardboard to eventually ignite. Note that the cardboard of an adjacent dwelling is typically exposed to these heat fluxes as a result of poor construction methods, or gaps as a result of the flutes [19]. This finding is similar to [53] but is slightly less conservative than [19] that found that a safe separation distance should be 3.8 m. In [19] the calculations to estimate the safe separation distance was made by using the maximum heat flux values, rather than the steady state values, in Beer's Law. The findings would be very similar should one use the average steady state heat flux values in the equations used by [19].

Since FDS demonstrated its ability to match the experimental results for the timber clad ISD, the model's predictive capabilities can be used estimate a preliminary critical separation distance between timber ISDs. Following the same logic as for the steel clad section, Eq. 5 gives $\overline{\ln(M/E)} = 0.11$. The scatter plot of model predictions and experimental measurements for the timber clad dwelling are depicted in Fig. 32.

Using $\overline{\ln(M/E)} = 0.11$ in Eqs. 6 and 8, gives a model standard deviation of 0.09 and a model bias factor of 1.06, indicating that the model tends to overpredict by 6% on average. Using Eq. 9, $\mu = 7.45$, $\sigma = 0.68$, assuming a critical heat flux for fire spread to occur as 8.5 kW/m^2 and using a predicted heat flux of M = 7.9 kW/m^2 (i.e. as predicted by the FDS model at 3 m from the door at Level A), the chance that the CHF of cardboard is exceeded at a distance of 3 m is 6%, based on these FDS model predictions. This indicates that it is unlikely for fire spread to occur at 3 m. It should be noted that if the wind conditions become unfavorable this finding will be different.

8. Conclusion

This paper has discussed the issues related to, or contributing to, fires in informal settlements and the lack of understanding pertaining to fire dynamics in ISDs and numerical modelling of ISDs. The paper focused on demonstrating numerical

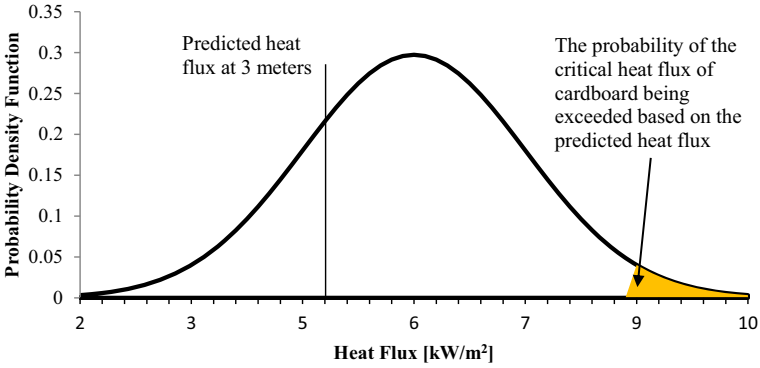

Figure 31. Probability of fire spread occurring at 3 m spacing, between door opening and the adjacent dwelling. Note that the critical heat flux where fire spread could occur is assumed to be the critical heat flux of cardboard (i.e. one of the most common lining materials in informal settlements).

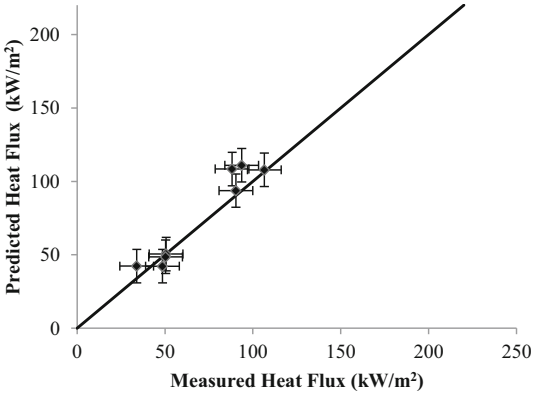

Figure 32. Scatter plot of model predictions and experimental measurements for the timber clad dwelling.

models against full scale experiments, and using the models developed to predict a critical separation distance between dwellings. The paper showed that there are challenges to demonstrate the compartment fire behaviour, with FDS, without experimental data (i.e. heat flux and temperatures from the experiments). It shows the complication surrounding compartment fires where leakages are present, and difficulties associated with sudden changes in ventilation conditions (e.g. timber cladding burning), and how these unique phenomena affect the estimation of heat fluxes to the surrounding environment. The predicted two-zone models gas temperatures showed good correlation to the experimental gas temperatures. However, the OZone models were limited and cannot predict heat fluxes, which is crucial when trying to understand fire spread behaviour in informal settlements.

Additionally, OZone limits the number of openings per wall to 3, which is not ideal from dwellings with high wall porosity (i.e. like ISDs).

Two full-scale burn experiments have been conducted on ISDs looking at the difference between timber and steel clad dwellings. It was found that temperatures in an ISD can reach 1000–1150°C depending on the total fuel load (i.e. including the structure). The maximum heat fluxes experienced were relatively similar for the steel and timber dwelling, where the steel clad dwelling had an average heat flux at the window (Level A) and the door (Level B) of 80 kW/m^2 and 88 kW/m^2, respectively and the timber clad dwelling had an average heat flux at window (Level A) and door (Level A) of 88 kW/m^2 and 93 kW/m^2, respectively. It is clear that the heat fluxes experienced for both the timber and steel clad dwelling are extremely high and a result a minimum separation distance of 3 m should be kept between these dwellings. However, this is not always possible because of socio-economic issues.

Based on the given input parameters used in the FDS models in this work, it was found that at a separation distance of 3 m that there was a 3.3% and a 6% chance that the heat flux would exceed the critical heat flux of cardboard for the steel clad and timber clad dwelling, respectively. It should be noted that this is only applicable for the experiments done in this work and that factors such as wind and different fuel load will affect the critical separation distance.

As a result of the complex nature of ISDs, social particularities and inherently unregulated environments, significant challenges are confronted when developing interventions for informal settlements. Thus, the problems cannot be identified, isolated and solved in a similar manner than commercial buildings or formal dwellings. However, with more than one billion people residing in informal settlements it is a cause for serious concern, and there is a significant need to understand and improve fire safety in informal settlements.

Acknowledgements

The authors would like to gratefully acknowledge Breede Valley Fire Department, especially Mr. J.J. Pretorius and T. Botha and their team, for their contribution and assistance towards helping the authors successfully complete the experiments. This work has been assisted by the Western Cape Disaster Management, Fire & Rescue Services, especially Mr. Rodney Eksteen. The authors would like to acknowledge the financial support of the Cape Higher Education Consortium & Western Cape Government (CHEC-WCG) partnership, the Ove Arup Foundation (TOAF), the Global Challenges Research Fund (GCRF of the EPSRC) under Unique Grant Number EP/P029582/1, and the Lloyd's Register Foundation under the "Fire Engineering Education for Africa" grant. Computations were performed using the University of Stellenbosch's HPC1: http://www.sun.ac.za/hpc and the University of Edinburgh's HPC Eddiehttps://www.ed.ac.uk/information-services/research-support/research-computing/ecdf/high-performance-computing.

Open Access

References

1. Mock C, Peck M, Krug E, Haberal M (2009) Confronting the global burden of burns: a WHO plan and a challenge. Burns 35:615–617. https://doi.org/10.1016/j.burns.2008.08.016
2. DMFRS (2015) Western Cape Strategic Framework for Fire and Burn Injury Prevention. Western Cape Strategic Framework for Fire and Burn Injury Prevention. Western Cape Disaster Management and Fire/Rescue Services, pp 8–32
3. Zweig P, Pharoah R, Eksteen R, Walls RS (2018) Installation of smoke alarms in an informal settlement community in Cape Town, South Africa. Final Report
4. Walls RS, Zweig P (2017) Towards sustainable slums: understanding fire engineering in informal settlements. In: Bahei-El-Din Y, Hassan M (eds) Advanced technologies for sustainable systems Springer, Cairo, pp 93–98. https://doi.org/10.1007/978-3-319-48725-0
5. Walls R, Olivier G, Eksteen R (2017) Informal settlement fires in South Africa: fire engineering overview and full-scale tests on ''shacks''. Fire Saf J 91:997–1006
6. UN-Habitat (2016) Slum Almanac 2015/2016: tackling improvement in the lives of Slum Dwellers, Nairobi
7. Ministry of Water Resources (1997) Disaster Review 1996, Kathmandu, Nepal
8. Baptist C, Bolnick J (2009) Participatory enumerations, in situ upgrading and mega events: the 2009 survey in Joe Slovo, Cape Town. Environ Urban 24(2012):59–66. https://doi.org/10.1177/0956247811435888
9. Owusu M (2013) Community-managed reconstruction after the 2012 fire in Old Fadama, Ghana. https://doi.org/10.1177/0956247812469928
10. Salinas-silva V (2015) The 'GREAT FIRE' of valparaiso 2014: social class differences and people' s vulnerability. a case study of wildland-urban fire. UCL Hazard Centre Disaster Studies and Management Working Paper no. 30 May 2015, London, UK
11. Kahanji C, Walls RS, Cicione A (2019) Fire spread analysis for the 2017 Imizamo Yethu informal settlement conflagration in South Africa. Int J Disaster Risk Reduct. https://doi.org/10.1016/j.ijdrr.2019.101146
12. McGrattan K, Hostikka S, McDermott R, Floyd J, Weinschenk C, Overholt K (2013) Fire dynamics simulator, Technical Reference Guide. NIST Special Publication 1018-1. https://doi.org/10.6028/nist.sp.1018-1
13. Emmerich SJ, McGrattan KB (1998) Application of a large eddy simulation model to study room airflow. ASHRAE Trans 104(1):1–9
14. Olson DB, Pickens JC, Gill RJ (2003) Numerical modeling of pool fires using LES and finite volume method for radiation. In: Seventh international symposium on fire safety science, vol 62. International Association for Fire Safety Science, pp 383–394. https://doi.org/10.1016/0010-2180(85)90092-6
15. Hietaniemi J, Hostikka S, Vaari J (2004) FDS simulation of fire spread—comparison of model results with experimental data. VTT Building and Transport, Espoo, Finland

16. Rein G, Torero JL, Jahn W, Stern J, Ryder NL, Desanghere S, Lázaro M, Mowrer F, Coles A, Joyeux D, Alvear D, Capote JA, Jowsey A, Reszka P (2007) A priori modelling of fire test one. In: Dalmarnock fire tests experiments and modelling, pp 173–192
17. Jahn W, Rein G, Torero JL (2007) A posteriori modelling of fire test one, the dalmarnock fire tests: experiments and modelling. The School of Engineering and Electronics, University of Edinburgh, pp 193–210. ISBN 978-0-9557497-0-4
18. Pope ND, Bailey CG (2006) Quantitative comparison of FDS and parametric fire curves with post-flashover compartment fire test data. Fire Saf J 41:99–110. https://doi.org/10.1016/j.firesaf.2005.11.002
19. Cicione A, Walls RS, Kahanji C (2019) Experimental study of fire spread between multiple full scale informal settlement dwellings. Fire Saf J 105:19–27. https://doi.org/10.1016/j.firesaf.2019.02.001
20. Cicione A, Walls RS (2019) Towards a simplified fire dynamic simulator model to analyse fire spread between multiple informal settlement dwellings based on full-scale experiments. In: 15th international conference and exhibition on fire science and engineering
21. Walls RS, Eksteen R, Kahanji C, Cicione A (2019) Appraisal of fire safety interventions and strategies for informal settlements in South Africa. Disaster Prev Manag 28(3):343–358. https://doi.org/10.1108/DPM-10-2018-0350
22. Moradi A (2016) Fire spreading in South African low-cost settlements ''A physics-based model''. Masters Thesis, Stellenbosch University, Stellenbosch
23. Khan MM, De Ris JL, Ogden SD (2008) Effect of moisture on ignition time of cellulosic materials. Fire Saf Sci 167–178. https://doi.org/10.3801/iafss.fss.9-167
24. Kim E, Dembsey N (2012) Engineering guide for estimating material pyrolysis properties for fire modeling. https://www.wpi.edu/sites/default/files/docs/Departments-Programs/Fire-Protection/WPI-Fire-Report-14-III.pdf
25. Cicione A, Walls R (2019) Estimating time to structural collapse of informal settlement dwellings based on structural fire engineering principles. In: SEMC conference. CRC Press
26. McGrattan K, Hostikka S, McDermott R, Floyd J, Weinschenk C, Overholt K (2013) Fire dynamics simulator user's guide. NIST Special Publication 1019-6. doi:http://dx.doi.org/10.6028/NIST.SP.1019
27. Forney GP (2018) Smokeview, A tool for visualizing fire dynamics simulation data volume I: user's guide
28. Mcgrattan K, Mcdermott R, Simo H, Floyd J, Vanella M, Weinschenk C, Overholt K (2017) Fire dynamics simulator technical reference guide volume 3: validation. NIST Special Publication 1018-3. 3
29. Babrauskas V (2016) Heat release rates. In: Hurley MJ (ed) et alSFPE handbook of fire protection engineering, 5th edn. Springer, Berlin, p 829. 10.1007/978-1-4939-2565-0
30. McGrattan KB, Baum HR, Rehm RG (1999) Large eddy simulations of smoke movement. Fire Saf J 105:161–178. https://doi.org/10.1016/S0379-7112(97)00041-6
31. Baum H, Mccaffrey B (1989) Fire induced flow field—theory and experiment. In: Fire safety science, pp 129–148. https://doi.org/10.3801/iafss.fss.2-129
32. Yang P, Tan X, Xin W (2011) Experimental study and numerical simulation for a storehouse fire accident. Build Environ 46:1445–1459. https://doi.org/10.1016/j.buildenv.2011.01.012
33. Floyd JE (2002) Comparison of CFAST and FDS for fire simulation with the HDR T51 and T52 tests
34. Merci B, Van Maele K (2008) Numerical simulations of full-scale enclosure fires in a small compartment with natural roof ventilation. Fire Saf J 43:495–511. https://doi.org/10.1016/j.firesaf.2007.12.003

35. Zhang S, Ni X, Zhao M, Feng J, Zhang R (2015) Numerical simulation of wood crib fire behavior in a confined space using cone calorimeter data. J Therm Anal Calorim 119:2291–2303. https://doi.org/10.1007/s10973-014-4291-4
36. Anderson J, Sjostrom J, Alastair T, Dai X, Welch S, Rush D (2019) FDS simulations and modelling efforts of travelling fires in a large elongated compartment. In: 15th international conference and exhibition on fire science and engineering, pp 2085–2094
37. CEN (2005) Eurocode 4—Design of composite steel and concrete structures—Part 1-2: General rules—Structural fire design
38. Tien CL, Lee KY, Stretton AJ (2016) Radiation heat transfer. In: SFPE handbook of fire protection engineering, 5th edn
39. Ren N, de Vries J, Zhou X, Chaos M, Meredith KV, Wang Y (2017) Large-scale fire suppression modeling of corrugated cardboard boxes on wood pallets in rack-storage configurations. Fire Saf J 91:695–704. https://doi.org/10.1016/j.firesaf.2017.04.008
40. Drysdale D (2011) An introduction to fire dynamics, 3rd edn. Wiley, New York
41. Radmanović K, Đukić I, Pervan S (2014) Specific heat capacity of wood. Drv. Ind. https://doi.org/10.5552/drind.2014.1333
42. Chaos M, Khan MM, Krishnamoorthy N, De Ris JL, Dorofeev SB (2011) Evaluation of optimization schemes and determination of solid fuel properties for CFD fire models using bench-scale pyrolysis tests. Proc Combust Inst 33:2599–2606. https://doi.org/10.1016/j.proci.2010.07.018
43. Robbins AP, Wade CA (2008) Soot yield values for modelling purposes—residential Occupancies
44. Tewarson A (2016) Generation of heat and chemical compounds in fires. In: DiNenno P (ed) SFPE handbook of fire protection engineering, 3rd edn, pp 277–324. https://doi.org/10.1007/978-1-4939-2565-0_9
45. Cadorin JF, Pintea D, Franssen JM (2001) The design fire tool OZONE V2.0—Theoretical description and validation on experimental fire tests
46. Mccaffrey BJ (1983) Momentum Implications for Buoyant Diffusion Flames. Combust Flame 52:149–167
47. Heskestad G (2002) Fire dynamics. In: SFPE handbook of fire protection engineering, 3rd edn. NFPA, pp 2-1–2-17
48. Thomas PH, Hinkley P, Theobald C, Simms DL (1963) Investigations into the flow of hot gases in roof venting. The Stationary Office, London
49. Zukoski EE (1994) Proceedings of the fourth IAFSS symposium. In: Proceedings of fourth IAFSS symposium, pp 137–147
50. Buchanan AH, Abu AK (2017) Structural design for fire safety, 2nd edn. Wiley, West Sussex
51. McGrattan K, Toman B (2011) Quantifying the predictive uncertainty of complex numerical models. Metrologia. 48:173–180. https://doi.org/10.1088/0026-1394/48/3/011
52. Peacock RD, Reneke PA, David WD, Jones WW (1999) Quantifying fire model evaluation using functional analysis. Fire Saf J 33:167–184
53. Wang Y, Gibson L, Beshir M, Rush D (2018) Preliminary investigation of critical separation distance between shacks in informal settlements fire. In: 11th Asia-Oceania symposium on fire science and technology